Syntheses and Multinuclear NMR Characterizations of α-$[SiMo_2W_9O_{39}]^{8-}$ and α-$[SiMo_{3-x}V_xW_9O_{40}]^{(4+x)-}$ (x = 1, 2) Heteropolyoxometalates†

Emmanuel Cadot, René Thouvenot, André Tézé,* and Gilbert Hervé

Laboratoire de Chimie des Métaux de Transition, Unité associée au CNRS 419, Université Pierre et Marie Curie, Case 42, 4, place Jussieu, 75252 Paris Cedex 05, France

Received March 25, 1992

The α-$[SiMo_{3-x}V_xW_9O_{40}]^{(4+x)-}$ (x = 1, 2) mixed heteropolyanions were obtained from A-α-$[SiW_9O_{34}]^{10-}$ by stereospecific synthetic routes via the monovacant α-$[SiMo_2W_9O_{39}]^{8-}$ anion. Structural analyses by ^{183}W NMR have proved that the structure of the A-α-$[SiW_9O_{34}]^{10-}$ subunit is retained in all these compounds. 2D COSY ^{183}W NMR has been applied to α-$[SiMo_2VW_9O_{40}]^{5-}$ in order to establish unambiguously the complete assignment. The magnitudes of the $^2J_{W-O-W}$ values are discussed with respect to the occupancy of sites 1–3 (vacancy, molybdenum(VI), or vanadium(V)), providing information about the deformations induced in the tungstic subunit. Also discussed are the ^{51}V line shape with respect to the respective peculiarities of the V–O–V, V–O–Mo, and V–O–W μ-oxo bridges and a correlation between the line broadenings of ^{51}V and ^{183}W.

Introduction

Mixed heteropolyanions (HPA) containing vanadium atoms were extensively studied in the last decade, mostly because of their potential use as oxidation catalysts, in homogeneous as well as in heterogeneous reactions.[1] Efficiencies of vanadomolybdophosphoric acids $H_{3+x}[PMo_{12-x}V_xO_{40}]$ in oxidation of alcohols,[2] methacrolein,[3] and isobutyric acid[4] were studied, and activities and selectivities were compared by following the x value (1–3). Such comparisons must be taken with caution, however, since usual methods of preparation starting from a mixture of the mononuclear anions $[MoO_4]^{2-}$ and $[VO_4]^{3-}$ and acidification give mixtures containing species which differ in their composition and, for each global composition, in the distribution of the geometrical isomers. The distribution of species depends on the relative proportions of starting materials and, to a lesser extent, on the experimental conditions. The similarity between physicochemical properties of all components precludes the obtention of any pure heteropolyacid.

Compounds containing Mo and V atoms in well-defined positions in the Keggin structure can be obtained from polyvacant stable tungsten heteropolyanions to which molybdenum and vanadium atoms are added. These compounds can be used as models to check the influence of Mo and V atoms on their catalytic properties. In order to change the V:Mo ratio, at least a trivacant tungstic matrix is needed. The α-$[SiW_9O_{34}]^{10-}$ anion, deriving from the Keggin structure α-$[SiW_{12}O_{40}]^{4-}$, has been chosen as the more stable member of this class of compounds.[5]

This paper reports the preparation of α-$[SiMo_2VW_9O_{40}]^{5-}$, α-$[SiMoV_2W_9O_{40}]^{6-}$, and the monovacant α-$[SiMo_2W_9O_{39}]^{8-}$ and their structural characterization by multinuclear ^{51}V, ^{29}Si, and ^{183}W NMR. Also discussed are the deformations induced in the Keggin structure by the substitution of V atoms for W or Mo atoms. During the course of this work, a paper from a Chinese group appeared reporting powder X-ray diffraction data for some of these compounds.[6]

Experimental Section

NMR Measurements. The ^{183}W and ^{29}Si NMR spectra were recorded for nearly saturated aqueous solutions in a 10 mm o.d. tube on a Bruker WM 250 apparatus operating at 10.4 and 49.7 MHz, respectively. The solutions were prepared by dissolving the acid or Li^+ salt obtained through resin exchange. In the case of the lithium salt of the α-$[SiMo_2W_9O_{40}]^{8-}$ anion, an alternative procedure was used: its potassium salt was poured into an aqueous saturated $LiClO_4$ solution and the resulting $KClO_4$ precipitate filtered off. The spectral width for ^{183}W was generally about 1000–1200 Hz (about 100–120 ppm), allowing a digitalization better than 0.2 Hz/point after a 16K-point Fourier transformation and even a better digital resolution with more zero-filling prior to transformation. ^{51}V NMR spectra were recorded for dilute solutions (10^{-2} M) in a 10 mm o.d. tube on a Bruker WM 250 apparatus operating at 65.7 MHz.

The chemical shifts were measured with respect to an external 2 M Na_2WO_4 solution in alkaline D_2O for ^{183}W, using saturated dodecatungstosilicic acid (D_2O solution) as a secondary standard (δ = −103.8 ppm), to external neat TMS for ^{29}Si, and to neat $VOCl_3$ using a VO_4^{3-} solution in alkaline D_2O as a secondary standard (δ = −536 ppm) for ^{51}V.

The ^{183}W 2D COSY spectrum of α-$[SiMo_2VW_9O_{40}]^{5-}$ was run on the nearly saturated aqueous solution (acidic form) at an operating frequency of 15 MHz on an AM 360 Bruker apparatus. The time domain was 1K in the F_2 dimension for a spectral width of 1500 Hz. Sixty-four experiments of 2000 runs each were stored; the delay (1 s) before the first 90° pulse (37 μs) allowed the complete relaxation of the different tungsten nuclei.

Infrared spectra were recorded on a Perkin-Elmer 283 spectrometer using KBr pellets.

Analyses. Complete elemental analyses were performed only on the potassium salts from which the acid and solutions of the lithium salts were obtained. Water content was determined by thermal gravimetric analysis. Molybdenum, vanadium, and tungsten were determined by a polarographic method in the presence of pyrocatechol, and potassium was determined by gravimetric analysis. The silicon content was determined by the Laboratoire central d'analyse du CNRS.

Preparations of the Compounds. $K_8[\alpha$-$SiMo_2W_9O_{39}]\cdot 20H_2O$. Sodium molybdate (8.0 g; 33 mmol) and lithium chloride (2.5 g; 60 mmol) are dissolved in 60 mL of water. α-$Na_{10}SiW_9O_{34}\cdot 18H_2O$[5] (45 g; 16 mmol) is added to the stirred solution. A 4 M HCl solution (23 mL) is added. The pH is 5.0–5.5. Eventually, a trace amount of insoluble material is filtered off. The white potassium–lithium salt of α-$[SiMo_2W_9O_{39}]^{8-}$ is precipitated by addition of potassium chloride (12 g). In order to obtain a pure potassium salt, the crude product is precipitated again three times

† Presented in part at the 1989 International Chemical Congress of Pacific Basin Societies (PACIFICHEM'89), Honolulu, HI.

(1) For a review, see: Misono, M. *Catal. Rev.—Sci. Eng.* **1987**, *29*, 269 and references therein.
(2) Bielanski, A.; Pozniczek, J.; Malecka, A. *React. Kinet. Catal. Lett.* **1990**, *1*, 127.
(3) Misono, M.; Koyama, T.; Sekiguchi, H.; Yoneda, Y. *Chem. Lett.* **1982**, 53.
(4) Akimoto, M.; Ikeda, H.; Okabe, A.; Echigoya, A. *J. Catal.* **1984**, *89*, 196. (b) Haeberle, T.; Emig, G. *Chem. Eng. Technol.* **1988**, *11*, 392. (c) Watzenberger, A.; Emig, G.; Lynch, D. T. *J. Catal.* **1990**, *124*, 247.
(5) (a) Hervé, G.; Tézé, A. *Inorg. Chem.* **1977**, *16*, 2115. (b) Robert, F.; Tézé, A. *Acta Crystallogr., Sect. B: Struct. Crystallogr. Cryst. Chem.* **1981**, *B37*, 318.
(6) Zhu, J.; Wang, J.; Liu, H.; Chen, R. *Huaxue Tongbao* **1989**, 28–29; *Chem. Abstr.* **1990**, *112*, 150695a.

0020-1669/92/1331-4128$03.00/0

by the addition of solid potassium chloride (yield 35 g). Anal. Calcd for α-$K_8SiMo_2W_9O_{39}\cdot 20H_2O$: K, 9.83; Mo, 6.04; W, 52.00; H_2O, 11.34. Found: K, 9.88; Mo, 6.03; W, 51.08; H_2O, 11.68. IR (cm^{-1}): 910 (w), 945 (w), 890 (s), 795 (m), 730 (m), 512 (m), 465 (w), 365 (w), 330 (w).

$K_4[\alpha$-$SiMo_3W_9O_{40}]\cdot 5H_2O$. Sodium molybdate (8 g; 33 mmol) is dissolved in 70 mL of water. A 30-mL portion of 4 M HCl is added to the stirred solution. Then, $Na_{10}[\alpha$-$SiW_9O_{34}]\cdot 18H_2O$ (30 g; 10.8 mmol) is quickly added. The yellow potassium salt $K_4[\alpha$-$SiMo_3W_9O_{40}]$ is precipitated by addition of solid potassium chloride (14 g) to the stirred solution (yield 25 g, 80%). Anal. Calcd: K, 5.47; Si, 1.01; Mo, 10.07; W, 57.89; H_2O, 3.14. Found: K, 5.52; Si, 0.95; Mo, 10.3; W, 57.1; H_2O, 3.2. IR (cm^{-1}): 1012 (w), 959 (m), 918 (s), 888 (vw), 868 (vw), 775 (vs), 548 (m), 465 (vw), 408 (vw), 368 (m), 331 (m).

$K_5[\alpha$-$SiMo_2VW_9O_{40}]\cdot 10H_2O$. Sodium vanadate (4.8 g; 40 mmol) is dissolved in about 230 mL of water. This solution is acidified by 4 M HCl (45 mL). Then solid $K_8SiMo_2W_9O_{39}\cdot 20H_2O$ (120 g; 40 mmol) is slowly added to the vigorously stirred solution. The desired yellow potassium salt is precipitated by addition of solid potassium chloride (50 g). The product is filtered off, washed with a saturated potassium chloride solution, and air-dried (yield ~100 g, 84%). Anal. Calcd: K, 6.45; Si, 0.93; Mo, 6.33; V, 1.68; W, 54.58; H_2O, 8.90. Found: K, 6.74; Si, 1.00; Mo, 6.4; V, 1.62; W, 54.8; H_2O, 9.08. IR (cm^{-1}): 1007 (w), 962 (m), 913 (s), 874 (sh), 771 (vs), 530 (m), 470 (w), 370 (m), 330 (w).

$K_6[\alpha$-$SiMoV_2W_9O_{40}]\cdot 12H_2O$. The first step of preparation is the same as for $K_5[\alpha$-$SiMo_2VW_9O_{40}]$, but after dissolution of $K_8[\alpha$-$SiMo_2W_9O_{39}]$, 1 M acetic acid/1 M sodium acetate buffer (80 mL) and sodium vanadate (4.8 g dissolved in 80 mL of water) are added to the solution. The stirred solution is kept at 65 °C for 16 hours, and a constant volume is maintained. Then, the solution is cooled at about 0 °C. An orange potassium salt is precipitated by addition of potassium chloride (80 g). Crude product (~80 g, 65%) is collected and then is dissolved in 160 mL of water at about 50 °C. The salt slowly crystallizes at room temperature. Anal. Calcd: K, 7.89; Si, 0.94; Mo, 3.22; V, 3.42; W, 55.68; H_2O, 7.27. Found: K, 7.82; Si, 1.05; Mo, 3.2; V, 3.6; W, 53.1; H_2O, 7.24. IR (cm^{-1}): 1006 (w), 958 (m), 909 (s), 867 (sh), 767 (vs), 600 (vw), 535 (m), 475 (w), 370 (s), 330 (w).

$K_7[\alpha$-$SiV_3W_9O_{40}]\cdot 10H_2O$. Sodium vanadate (1.9 g; 15.5 mmol) is dissolved in 300 mL of water. To the stirred solution is added $Na_{10}[\alpha$-$SiW_9O_{34}]\cdot 18H_2O$ (145 g; 52 mmol), followed by 185 mL of 6 M sulfuric acid. Then, the solution is maintained under stirring for 45 min. The pH is adjusted between 6 and 7 by addition of solid potassium carbonate. An orange potassium salt (~100 g) is precipitated by addition of solid potassium chloride (80 g) and recrystallized in water. Anal. Calcd: K, 9.34; Si, 0.96; V, 5.16; W, 56.48; H_2O, 6.14. Found: K, 8.76; Si, 1.04; V, 5.2; W, 56.8; H_2O, 6.4.

Preparation of the Lithium Salts $Li_6[\alpha$-$SiMoV_2W_9O_{40}]$, $Li_7[\alpha$-$SiV_3W_9O_{40}]$, and $Li_8[\alpha$-$SiMo_2W_9O_{39}]$. The lithium salts are prepared from the corresponding potassium salts which are dissolved in water. Each solution is passed through a column of the Li form of a strongly acidic cation exchanger such as the Dowex 50W types, which are ring-sulfonated polystyrene resins. The resultant solution is evaporated to dryness.

Preparation of the Acids $H_{4+x}[\alpha$-$SiMo_{3-x}V_xW_9O_{40}]$ (x = 0–2). The potassium salts (15 g; 5 mmol) are each dissolved in 65 mL of water, and each solution is placed in a separatory funnel. Then diethyl ether is added, followed by a slow addition of concentrated hydrochloric acid (55, 85, or 100 mL for x = 0, 1, or 2, respectively). The heavy phase is collected and diethyl ether evaporated under vacuum. The resultant solid is dissolved in the minimum amount of water. Heteropolyacids slowly crystallize at room temperature.

Purities of lithium salts and acids were checked by electrochemical techniques and IR spectroscopy before recording NMR spectra.

Results

Formation of the Mixed HPA. Addition of molybdate on the trivacant anion α-$[SiW_9O_{34}]^{10-}$ gives, in acidic medium (pH 1–2), the Keggin structure species α-$[SiMo_3W_9O_{40}]^{4-}$. At higher pH (5–5.5), this reaction leads to α-$[SiMo_2W_9O_{39}]^{8-}$.[7] This monovacant anion further reacts, in acidic medium, with 1 equiv of tungstate, molybdate, or vanadate, giving the saturated anion α-$[SiMo_2W_{10}O_{40}]^{4-}$, α-$[SiMo_3W_9O_{40}]^{4-}$, or α-$[SiMo_2VW_9O_{40}]^{5-}$, respectively. Whatever the pH conditions, addition of vanadate

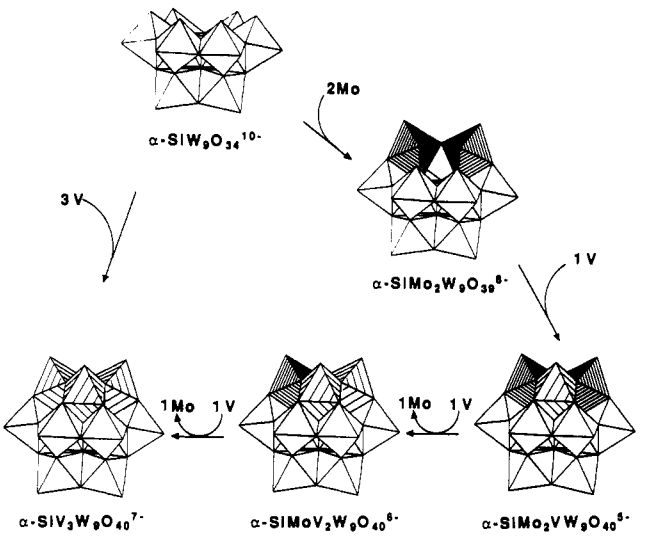

Figure 1. Interconversion processes involving α-$[SiW_9O_{34}]^{10-}$, α-$[SiMo_2W_9O_{39}]^{8-}$, and the mixed dodeca(molybdotungstovanado)silicates.

to α-$[SiW_9O_{34}]^{10-}$ gives only α-$[SiV_3W_9O_{40}]^{7-}$[8] because this anion is stable up to pH 10 and decomposes directly into tungstate and vanadate at higher pH. Thus, there is no monovacant precursor suitable to obtain α-$[SiMoV_2W_9O_{40}]^{6-}$ through direct addition of vanadate or molybdate. The only way to prepare the divanadium anion appeared then to be the substitution of one vanadium(V) for one molybdenum(VI) atom in the anion α-$[SiMo_2VW_9O_{40}]^{5-}$. This reaction is selective, in accordance with the higher lability of molybdenum compared to tungsten atoms.[9] Although the anion α-$[SiMoVW_9O_{39}]^{9-}$ has never been identified, the entire reaction can be tentatively described as a dissociative mechanism with formation of this monovacant anion as an intermediate.

An increased resistance to nucleophilic degradation of a Keggin anion results from increasing its negative charge. Consequently, in an appropriate pH range, the supposed monovacant intermediate α-$[SiMoVW_9O_{39}]^{9-}$ may add vanadium to give the divanadium anion α-$[SiMoV_2W_9O_{40}]^{6-}$, which is more stable than the monovanadium one.

Actually, α-$[SiMoV_2W_9O_{40}]^{6-}$ was prepared from the monovacant anion α-$[SiMo_2W_9O_{39}]^{8-}$, which quickly adds 1 mol of vanadate/mol in acidic medium (pH 1), giving in a first step α-$[SiMo_2VW_9O_{40}]^{5-}$ and then the divanadium anion, after increasing the pH, by the formal substitution process described above. These successive reactions were followed by polarography, each polyanion being identified by its first-wave potential. The best result was obtained when the reaction was carried out at pH 5.00 and 65 °C with the stoichiometric amount of sodium vanadate. The reaction routes for the preparation of mixed heteropolyoxometalates are summarized in Figure 1.

^{183}W NMR Characterizations. The complete assignments of the 1D spectra are based on an examination of the $^2J_{W\text{-}O\text{-}W}$ coupling constants, which allows us to derive the tungsten–tungsten connectivities. The coupling constant values depend on the W–O–W μ-oxo angles and the W–O bond lengths. Thus, for saturated Keggin anions, tungsten atoms sharing a common corner oxygen (angle about 150°) have $^2J_{W\text{-}O\text{-}W}$ values of about 15–22 Hz, while those edge shared (120° angle) present substantially smaller $^2J_{W\text{-}O\text{-}W}$ values in the 5–7-Hz range.[10] Moreover, in compounds with metallic vacancies, very small corner couplings (<10 Hz) are observed for coupling tungsten atoms in the vicinity

(7) Contant, R.; Fruchart, J. M.; Hervé, G.; Tézé, A. *C. R. Hebd. Seances Acad. Sci., Ser. C* **1974**, *278*, 199.

(8) Mossoba, M. M.; O'Connor, C. J.; Pope, M. T.; Sinn, E.; Hervé, G.; Tézé, A. *J. Am. Chem. Soc.* **1980**, *102*, 6864.

(9) Contant, R.; Ciabrini, J. P. *J. Inorg. Nucl. Chem.* **1981**, *43*, 1525.

(10) Lefebvre, J.; Chauveau, F.; Doppelt, P.; Brévard, C. *J. Am. Chem. Soc.* **1981**, *103*, 4589.

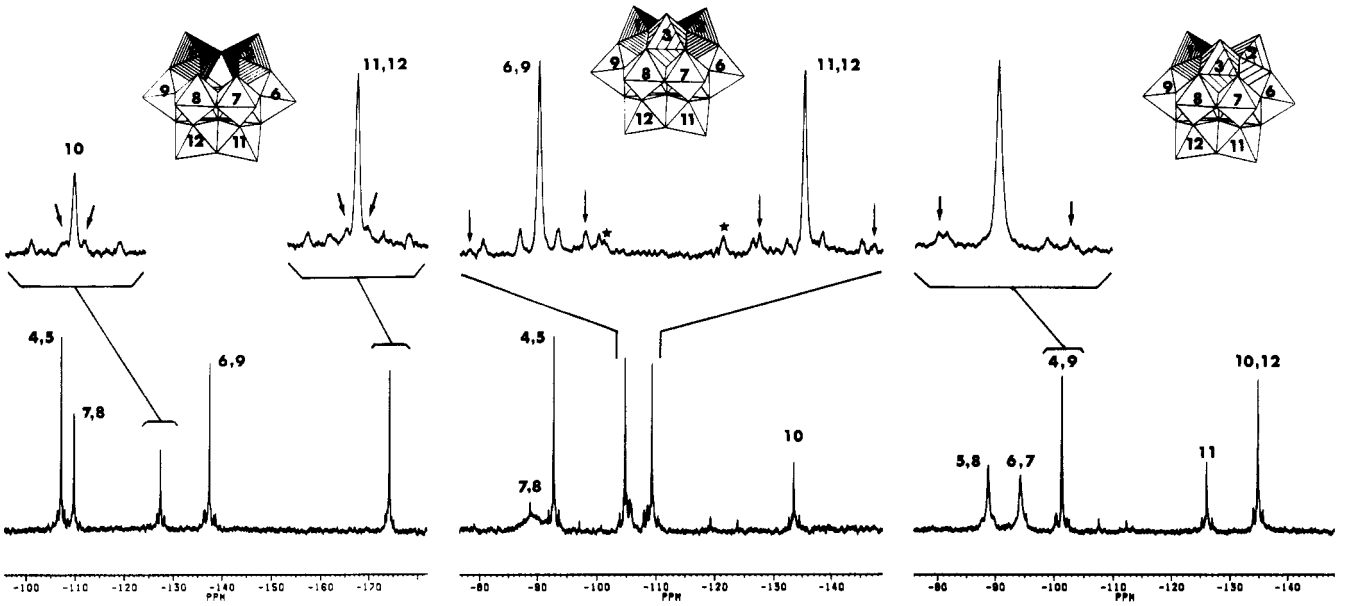

Figure 2. 10.4-MHz ^{183}W NMR spectra and polyhedral representations with the IUPAC numbering of (a, left) α-$[SiMo_2W_9O_{39}]^{8-}$ (aqueous solution of Li^+ salt), with the expanded part showing the very low edge coupling constant (3.8 Hz; satellites marked by arrows) between W_{10} and $W_{11}(W_{12})$, (b, middle) α-$[SiMo_2VW_9O_{40}]^{5-}$ (acidic form in aqueous solution), with the expanded part showing the mutual corner coupling constant (20.2 Hz; AB system; satellites marked by arrows) between $W_6(W_9)$ and $W_{11}(W_{12})$, and (c, right) α-$[SiMoV_2W_9O_{40}]^{6-}$ (aqueous solution of Li^+ salt), with the expanded part showing the AB system for the satellites (marked by arrows) of the $W_4(W_9)$ line (−101.3 ppm).

of the vacancy. This difference with respect to the saturated anions has been explained by the existence of a large W–O bond, where the bridging oxygen atom is trans to a terminal one.[11]

In addition, the relative intensity of the $^2J_{W\text{-}O\text{-}W}$ satellite gives the number of the tungsten atoms coupled to the observed nuclei. Last, the lines of the tungsten atoms adjacent to vanadium atoms are broadened with respect to the other lines ($\Delta\nu_{1/2} \approx 1$ Hz), and the width of the resonance line depends on the quadrupolar relaxation of the ^{51}V nucleus and on the $^2J_{V\text{-}O\text{-}W}$ coupling constant.[12]

The ^{183}W NMR spectra with the corresponding structures and IUPAC numbering[13] are shown in Figure 2. The spectral data are reported in Table I.

α-$[SiMo_2W_9O_{39}]^{8-}$. The ^{183}W NMR spectrum of the $Li_8[\alpha$-$SiMo_2W_9O_{39}]$ solution reveals five well-resolved resonance lines with an intensity ratio of 2:2:1:2:2, in accordance with nine tungsten atoms involved in the expected structure (C_s symmetry). With the vacancy in position 3, the five equivalent tungsten groups are numbered $W_4(W_5)$, $W_6(W_9)$, $W_7(W_8)$, W_{10}, $W_{11}(W_{12})$. On the basis of its intensity, the −127.8 ppm line is assigned to the unique tungsten W_{10}. This line exhibits a corner coupling ($^2J_{W\text{-}O\text{-}W}$ = 15.9 Hz) which allows it to connect to the −107.2 ppm line, then attributed to $W_4(W_5)$. The edge coupling constant ($^2J_{W\text{-}O\text{-}W}$ = 3.8 Hz) observed for both lines at −127.8 ppm (W_{10}) and at −174.8 ppm is unambiguously due to W_{10}–W_{11} and W_{10}–W_{12} junctions. So the −174.8 ppm line is attributed to $W_{11}(W_{12})$. In the same way, the peak at −107.2 ppm (W_4, W_5) is correlated with the −137.8 ppm line by an edge coupling constant ($^2J_{W\text{-}O\text{-}W}$ = 5.8 Hz). The peak at −137.8 ppm is then assigned to $W_6(W_9)$. The assignment of the remaining line at −110.1 ppm to $W_7(W_8)$ is further confirmed by the relatively low corner coupling constant ($^2J_{W\text{-}O\text{-}W}$ = 9.5 Hz) also observed for the $W_{11}(W_{12})$ line at −174.8 ppm. Such low corner coupling has been observed in polyvacant polyoxotungstates[11] for the W–O–W μ-oxo bridges with large W–O bonds where the junction oxygen atom is trans to a terminal oxygen atom. Actually, the $W_7(W_8)$ atom, adjacent to the vacancy, carries a second terminal oxygen atom. On the contrary, a large corner coupling is observed for the junction W_6–W_7 and W_8–W_9, which likely denotes a relatively short W–O bond or/and a large μ-oxo angle.[11] The $W_7(W_8)$ line appears significantly broader ($\Delta\nu_{1/2} \approx 1.2$ Hz) than the other lines ($\Delta\nu_{1/2} \approx 0.8$ Hz). This observation can be related to a more efficient chemical shift anisotropy relaxation for the tungsten atom $W_7(W_8)$ near the lacuna, which carries two cis terminal oxygen atoms in its coordination sphere. The complete assignments are summarized in Table Ia.

Table I. ^{183}W NMR Data (ppm and Hz) for (a) α-$[SiMo_2W_9O_{39}]^{8-}$, (b) α-$[SiMo_2VW_9O_{40}]^{5-}$, and (c) α-$[SiMoV_2W_9O_{40}]^{6-}$ (Chemical Shift Connectivity Matrix)

(a) α-$[SiMo_2W_9O_{39}]^{8-}$

	$W_4(W_5)$	$W_7(W_8)$	W_{10}	$W_6(W_9)$	$W_{11}(W_{12})$
$W_4(W_5)$	−107.2		15.9	5.8	
$W_7(W_8)$		−110.1		25.9	9.5
W_{10}	15.9		−127.8		3.8
$W_6(W_9)$	5.8	25.9		−137.8	18.4
$W_{11}(W_{12})$		9.5	3.8	18.0	−174.8

(b) α-$[SiMo_2VW_9O_{40}]^{5-}$

	$W_7(W_8)$	$W_4(W_5)$	$W_6(W_9)$	$W_{11}(W_{12})$	W_{10}
$W_7(W_8)$	−90		*a*	*a*	
$W_4(W_5)$		−93.4	6.8		18.3
$W_6(W_9)$	20.2	6.6	−105.3	20.2	
$W_{11}(W_{12})$	19.3		20.2	−109.4	6.6
W_{10}		18.6		6.3	−134.8

(c) α-$[SiMoV_2W_9O_{40}]^{6-}$

	$W_5(W_8)$	$W_6(W_7)$	$W_4(W_9)$	W_{11}	$W_{10}(W_{12})$
$W_5(W_8)$	−88.9	*a*	*a*		*a*
$W_6(W_7)$	*a*	−94.4		*a*	
$W_4(W_9)$	23.4		−101.3		18.1
W_{11}		17.8		−126.1	6.1
$W_{10}(W_{12})$	16.8		17.6	5.9	−134.8

[a] Coupling satellites cannot be determined due to the overlapping with the main resonance line which is broadened by proximity of vanadium atoms.

α-$[SiMo_2VW_9O_{40}]^{5-}$. The spectrum consists of five resonance lines in a ratio of 2:2:2:2:1, corresponding to nine tungsten atoms

(11) (a) Contant, R.; Hervé, G.; Thouvenot, R. Presented at the CNRS-NSF Workshop on Polyoxometalates, Saint-Lambert des Bois, France, 1983. (b) Canny, J.; Tézé, A.; Thouvenot, R.; Hervé, G. *Inorg. Chem.* **1986**, *25*, 2114. (c) Thouvenot, R.; Tézé, A.; Contant, R.; Hervé, G. *Inorg. Chem.* **1988**, *27*, 524.
(12) Domaille, P. J. *J. Am. Chem. Soc.* **1984**, *106*, 7677.
(13) Jeannin, Y.; Fournier, M. *Pure Appl. Chem.* **1987**, *59*, 1529.

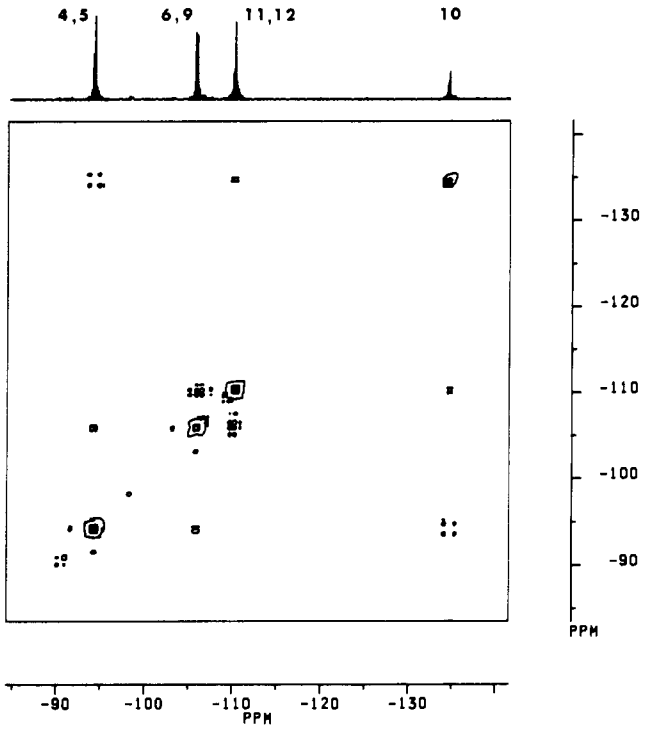

Figure 3. 15-MHz ^{183}W NMR 2D COSY spectrum of α-$[SiMoV_2W_9O_{40}]^{6-}$.

in a structure of C_s symmetry. As only one ^{183}W resonance (−90 ppm) appears relatively large ($\Delta\nu_{1/2}$ = 25 Hz), only two tungsten atoms are adjacent to the vanadium atom; its two other neighbors are necessarily the two molybdenum atoms of the anion. Furthermore, the spin–spin coupling parameters of the experimental spectrum and an examination of their connectivities show that the structure of α-$[SiW_9O_{34}]^{10-}$ is maintained throughout the successive addition of Mo and V atoms.

On the basis of its broadening, the high-frequency peak at −90 ppm is attributed to $W_7(W_8)$ adjacent to the ^{51}V quadrupolar nucleus. The low-frequency peak (−134.8 ppm) of relative intensity 1 is assigned to the unique tungsten atom W_{10}. This peak presents an edge coupling of 6.3 Hz and a corner coupling of 18.6 Hz due to the junctions with $W_{11}(W_{12})$ and $W_4(W_5)$, respectively. The possible corner coupling partner of the W_{10} line could be the −93.4 ppm line, which exhibits a similar corner coupling value ($^2J_{W\text{-}O\text{-}W}$ = 18.3 Hz). This line would then be attributed to $W_4(W_5)$. Confirming this assignment, intensities of the satellites proved that the involved atoms share only one corner bridge, a situation exclusively encountered in the case of $W_4(W_5)$. The $W_6(W_9)$ and $W_{11}(W_{12})$ pairs are expected to exhibit the same coupling pattern, i.e. two corner and one edge couplings actually observed on the −105.3 and −109.4 ppm lines. Moreover $W_6(W_9)$ and $W_{11}(W_{12})$ are mutually coupled by a corner junction, leading to an AB system ($^2J_{W\text{-}O\text{-}W}$ = 20.2 Hz; $\Delta\nu$ = 41.6 Hz at 10.4 MHz) for the satellites observed about both lines. Unfortunately, it is impossible to establish the correlation between these lines and the −134.8 and −93.4 ppm lines because of the near degeneracy of edge coupling observed on all these peaks ($^2J_{W\text{-}O\text{-}W} \approx 6.5$ Hz). Therefore, discrimination between the resonances of $W_{11}(W_{12})$ and $W_6(W_9)$ requires a 2D correlation spectrum.

The 2D COSY spectrum of α-$[SiMo_2VW_9O_{40}]^{5-}$ is shown as a contour plot in Figure 3. It confirms the assignment previously obtained. In addition, the lines at −105.3 and −109.4 ppm are clearly connected respectively to the −93.4 and −134.8 ppm lines, in both cases by edge coupling. Therefore the −105.3 ppm line was assigned to the $W_6(W_9)$ pair and the −109.4 ppm line to the $W_{11}(W_{12})$ pair. Let us note that the cross-peaks of $W_7(W_8)$ with $W_{11}(W_{12})$ and with $W_6(W_9)$ are not observed because of the broadness of the $W_7(W_8)$ resonance.

Table II. AB System (Hz) for the Tungsten–Tungsten Satellites of the α-$[SiMoV_2W_9O_{40}]^{6-}$ Anion for ν_B = −1056.7 Hz and $^2J_{W\text{-}O\text{-}W}$ = 23.4 Hz

ν_A	ν_1	$\Delta\nu_1$[a]	ν_2	$\Delta\nu_2$[a]
		Calculated		
−926.7	−1046.04	10.66	−1069.44	12.74
−983.8	−1046.83	9.87	−1070.23	13.53
		Observed		
	−1046	10.7[b]	−1069.4	12.7[b]

[a] $\Delta\nu_1 = \nu_1 - \nu_B$; $\Delta\nu_2 = \nu_B - \nu_2$. [b] ±0.1 Hz.

α-$[SiMoV_2W_9O_{40}]^{6-}$. The spectrum of $[SiMoV_2W_9O_{40}]^{6-}$ reveals five resonance lines with a relative ratio of 2:2:2:1:2, consistent with a C_s symmetry structure. Among these five peaks, the presence of two large peaks at high frequencies (−88.9 ppm, $\Delta\nu_{1/2}$ = 4 Hz; −94.4 ppm, $\Delta\nu_{1/2}$ = 6 Hz) allows us to conclude that the two equivalent vanadium and the molybdenum atoms are necessarily adjacent. On the basis of its intensity, the −126.1 ppm line is assigned to W_{11}, which is edge coupled with W_{10}-(W_{12}) ($^2J_{W\text{-}O\text{-}W}$ = 6.1 Hz) and is corner coupled to $W_6(W_7)$ ($^2J_{W\text{-}O\text{-}W}$ = 17.8 Hz). Owing to its coupling pattern, the −101.3 ppm line (no edge coupling and two corner couplings) and the −134.8 ppm line (one edge coupling and two corner couplings) are unambiguously identified respectively as $W_4(W_9)$ and W_{10}-(W_{12}), which are mutually corner coupled ($^2J_{W\text{-}O\text{-}W}$ = 17.8 ± 0.3 Hz). In addition to the coupling with $W_{10}(W_{12})$, the −101.3 ppm line (ν_B = −1056.7 Hz at 10.4 MHz) exhibits another pair of satellites as an AB system ($^2J_{W\text{-}O\text{-}W}$ = 23.4 Hz; ν_1 = −1046.0 Hz; $\Delta\nu_1 = \nu_1 - \nu_B$ = 10.7 Hz; ν_2 = −1069.4 Hz; $\Delta\nu_2 = \nu_B - \nu_2$ = 12.7 Hz; see Figure 2c).

Calculation of the AB system frequencies allows us to discriminate between the two possible coupling partners, either the line at −88.9 ppm (ν_A = −926.7 Hz) or that at −94.4 ppm (ν_A = −983.8 Hz). The frequencies of the satellites calculated according to the classical formulas

$$\nu_1 = {}^1/_2(\nu_A + \nu_B + J - \sqrt{(\nu_A - \nu_B)^2 + J^2})$$

$$\nu_2 = {}^1/_2(\nu_A + \nu_B - J - \sqrt{(\nu_A - \nu_B)^2 + J^2})$$

are reported in Table II for both ν_A values. Agreement is obtained for the −88.9 ppm line, which can be attributed with confidence to the $W_5(W_8)$ atom, and the remaining large line at −94.4 ppm is then assigned to $W_6(W_7)$. Let us remark that shoulders are seen (frequency separation about 20 Hz) at the foot of the −88.9 ppm line, corresponding to two pairs of unresolved tungsten satellites with corner coupling constants of 23.4 (with W_4–W_9) and 16.8 Hz (with W_{10}–W_{12}).

Discussion

The NMR studies of Keggin heteropolytungstates have shown that the magnitudes of the homonuclear $^2J_{W\text{-}O\text{-}W}$ coupling constants fall into two narrow ranges: 21–22 Hz for corner coupling and 5–7 Hz for edge coupling.[10] However, compounds with metallic vacancies exhibit a larger distribution of coupling constant values. For example, the spectrum of the monovacant anion α-$[SiW_{11}O_{39}]^{8-}$ shows corner coupling constants ranging from 9 to 26 Hz.[11a] When tungsten(VI) is replaced by a metal of lower oxidation state as in α-$[PTi_2W_{10}O_{40}]^{7-}$ or $[SiV_2W_{10}O_{40}]^{6-}$, a similar effect has been observed, though to a less extent compared to the case of vacant compounds.[14-16] The determination of the W–W coupling constants can yield information about the

(14) Knoth, W. H.; Domaille, P. J.; Roe, D. C. *Inorg. Chem.* **1983**, *22*, 198.
(15) Domaille, P. J.; Knoth, W. H. *Inorg. Chem.* **1983**, *22*, 818.
(16) Canny, J.; Thouvenot, R.; Tézé, A.; Hervé, G.; Leparulo-Loftus, M. A.; Pope, M. T. *Inorg. Chem.* **1991**, *30*, 976.

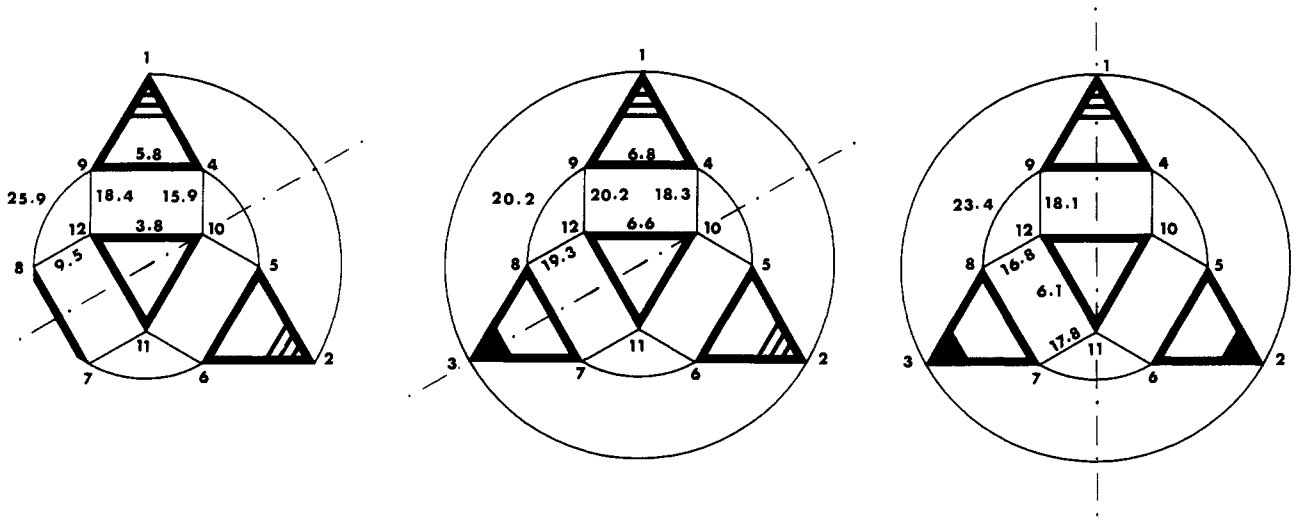

Figure 4. Schematic flat representation of the Keggin polyanions (a, left) α-$[SiMo_2W_9O_{39}]^{8-}$, (b, middle) α-$[SiMo_2VW_9O_{40}]^{5-}$, and (c, right) α-$[SiMoV_2W_9O_{40}]^{6-}$ and numbering of the metal atoms according to the IUPAC recommendations.[13] Atoms belonging to the same skeletal plane are disposed on a circle: 1–3 for plane A; 4–9 for plane B; 10–12 for plane C. Heavy lines represent edge junctions and light lines corner junctions. Each atom (except 1,2 and 7,8 in the monovacant $SiMoV_2W_9$ species) is then at the origin of two mutually cis corner junctions and two mutually cis edge junctions. Oxygen atoms and the central silicon atom are not represented. Molybdenum and vanadium atoms in locations 1–3 correspond to hatched and black triangles, respectively. The dotted line symbolizes the trace of the symmetry plane. Homonuclear coupling constants $^2J_{W\text{-}O\text{-}W}$, noted near the tungsten tungsten junctions, are given in hertz.

Table III. Experimental $^2J_{W\text{-}O\text{-}W}$ Corner Coupling Constants (Hz) for α-$[SiMo_2W_9O_{39}]^{8-}$, α-$[SiMo_3W_9O_{40}]^{4-}$, α-$[SiMo_2VW_9O_{40}]^{5-}$, α-$[SiMoV_2W_9O_{40}]^{6-}$, and α-$[SiV_3W_9O_{40}]^{7-}$: In-Plane $^2J_{B\text{-}B}$ between Tungsten Atoms Belonging to the Same Skeletal Plane B and Interplane $^2J_{B\text{-}C}$

	$^2J_{B\text{-}B}$	$^2J_{B\text{-}C}$	$^2J_{B\text{-}C}$(mean)
α-$SiMo_3W_9O_{40}^{4-}$		21.6	21.6
α-$SiMo_2VW_9O_{40}^{5-}$	20.2	18.4, 19.3, 20.2	19.3
α-$SiMoV_2W_9O_{40}^{6-}$	23.4	16.8, 17.8, 17.8	17.5
α-$SiV_3W_9O_{40}^{7-}$		16.0	16.0
α-$SiMo_2W_9O_{39}^{8-}$	25.9	9.5, 15.9, 18.2	14.5

deformations induced in the tungstic part of the structure by the addition of Mo and V atoms.

According to the IUPAC representation,[13] the metallic centers of the Keggin anion are located in three planes (Figure 4): plane A containing the three addenda atoms (sites 1–3), plane B containing the six tungsten atoms numbered 4–9, and plane C constituted by a tungstic triad involving atoms 10–12. The corner coupling constants can be arranged in two groups: corner coupling $^2J_{B\text{-}B}$ between tungsten atoms belonging to plane B and interplane corner coupling $^2J_{B\text{-}C}$ between tungsten nuclei located in planes B and C. For the symmetrical anions α-$[SiMo_3W_9O_{40}]^{4-}$ and α-$[SiV_3W_9O_{40}]^{7-}$ (C_{3v}), only $^2J_{B\text{-}C}$ coupling is observed (see Table III). Owing to the C_s symmetry of the three investigated compounds, only one $^2J_{B\text{-}B}$ value and three $^2J_{B\text{-}C}$ values are obtained from the ^{183}W spectra. It can be noted that the highest value for $^2J_{B\text{-}B}$ (25.9 Hz in α-$[SiMo_2W_9O_{39}]^{8-}$) is accompanied by the lowest value for $^2J_{B\text{-}C}$ (9.5 Hz). But, at this point, it appears more convenient to compare the mean value of $^2J_{B\text{-}C}$ to the $^2J_{B\text{-}B}$ coupling constant for each compound. As the mean value of $^2J_{B\text{-}C}$ decreases from 19.3 to 14.5 Hz, $^2J_{B\text{-}B}$ exhibits an opposite trend: it increases regularly from 20.2 to 25.9 Hz. These variations reflect some distortions induced in the α-$[SiW_9O_{34}]^{10-}$ subunit by the progressive Mo/V substitution. The largest distortion is observed in the monovacant dimolybdenum anion. The perturbation of the coordination sphere of the tungsten W_8 close to the vacancy implies strong alteration of the μ-oxo junctions ($^2J_{W_8\text{-}W_{12}}$ = 9.5 Hz and $^2J_{W_8\text{-}W_9}$ = 25.9 Hz). As discussed above, the small corner coupling $^2J_{W_8\text{-}W_{12}}$ is explained by a large W–O bond length trans to a short double bond W_8=O,[11b] whereas the large coupling could be due to a short W_8–W_9 bond or/and an opening of the W_8–O–W_9 bridge. The small edge coupling W_{10}–W_{12} (3.8 Hz) may also be related to a W–O bond larger than

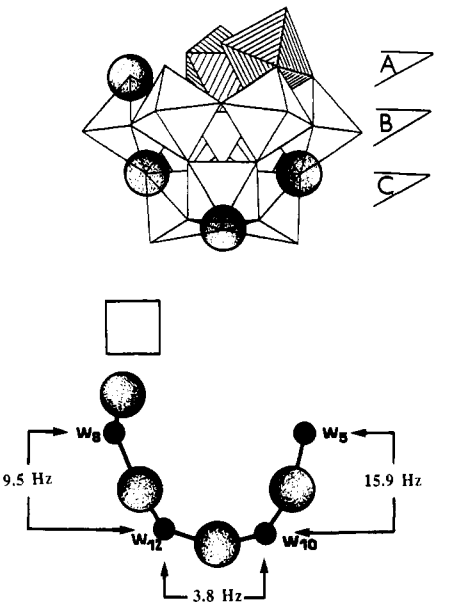

Figure 5. Concerted displacements of tungsten atoms along the successive μ-oxo bonds in α-$[SiMo_2W_9O_{39}]^{8-}$.

usual. In this edge junction, one oxygen atom is trans to a bridging oxygen atom which is itself trans to a terminal oxygen atom (Figure 5). In the same way, the junction W_5–W_{10} displays a significantly low corner coupling constant (15.9 Hz).

Such an accumulation of low coupling constants in this monovacant compound can be explained by a concerted displacement of all the involved tungsten atoms inside their coordination sphere leading to a successive alternation of short and long W–O bonds. A damping of this distortion is however observed along the W_8–W_{12}–W_{10}–W_5 chain as the distance from the perturbation site, i.e. the vacancy, increases. The concerted displacements of tungsten atoms along the successive μ-oxo-bonds is depicted in Figure 5. When the vacant metallic site is filled with V^V or Mo^{VI}, the main effect appears to be a shrinking of the distribution of the coupling constants corresponding to a decrease of the distortions. In particular, the $^2J_{W_8\text{-}W_{12}}$ coupling constant, involving one oxygen atom trans to the vacancy, increases from 9.5 to 19.3 Hz and to 21.6 Hz in α-$[SiMo_2VW_9O_{40}]^{5-}$ and α-$[SiMo_3W_9O_{40}]^{4-}$, respectively. This latter observation means

that the trans influence induced by the vacancy is strongly reduced by insertion of V^V and canceled by Mo^{VI}. When α-$[SiMo_2VW_9O_{40}]^{5-}$ and α-$[SiMoV_2W_9O_{40}]^{6-}$ are compared, it appears that the substitution of a second vanadium for one molybdenum leads to a decrease of $^2J_{W_8-W_{12}}$ from 19.3 to 16.8 Hz, showing a cumulative trans influence, exerted by the V–O–V bridge. The replacement of the last molybdenum atom by a third vanadium reinforces this trend, as the unique $^2J_{B-C}$ coupling for α-$[SiV_3W_9O_{40}]^{7-}$ (16 Hz) is significantly smaller than the $^2J_{B-C}$ mean value for α-$[SiMoV_2W_9O_{40}]^{6-}$ (17.5 Hz; see Table III). Therefore, in α-$[SiV_3W_9O_{40}]^{7-}$, the W–O bond of the W–O–V junction could be short and could alternate with a long V–O bond. In an alternative description of oxygen atoms in close contact, the three vanadium atoms would be displaced, shortening the V–V distance with respect to the V–W and V–Mo distances.

^{51}V NMR Line Width. As already observed for other vanadium-substituted Keggin[12,17,18] and Dawson[17] heteropolytungstates, the line width of the ^{51}V resonance increases with the number of adjacent vanadium atoms in the polyanion (100, 250, and 450 Hz for the unprotonated α-$[SiMo_2VW_9O_{40}]^{5-}$, α-$[SiMoV_2W_9O_{40}]^{6-}$, and α-$[SiV_3W_9O_{40}]^{7-}$ anions in diluted aqueous solutions, respectively). The line width of the quadrupolar ^{51}V nucleus is essentially governed by the quadrupolar relaxation according to

$$\pi(\Delta\nu_{1/2}) = T_{1q}^{-1} = T_{2q}^{-1} = \frac{3\pi^2}{10}\frac{2I+3}{I^2(2I-1)}\left[\frac{e^2q_{zz}Q}{h}\right]^2\left(1+\frac{1}{3}\eta^2\right)\tau_c$$

where q_{zz} and η characterize the electric field gradient tensor at the resonant nucleus (q_{zz} is the largest component of the efg, and η is the asymmetry parameter defined by $\eta = (q_{yy}-q_{xx})/q_{zz}$), eQ is the nuclear quadrupole moment, and τ_c is the correlation time for reorientation of the anion.

As the number of vanadium atoms in the polyoxoanion increases, there is likely no dramatic change in the correlation time τ_c and the increase of the ^{51}V relaxation rate should be related to an increase of the electric field gradient at the vanadium nucleus. The large relaxation time observed with the vanadium nucleus in monovanadium anions (narrow resonance line) is the consequence of a small electric field gradient at the center of the octahedral cavity. On the other hand, the shorter relaxation times observed with the di- and trivanadium anions can be related to a larger efg at the location of the adjacent vanadium nuclei, that is to say a greater distortion of the VO_6 octahedra, in agreement with our above conclusions.

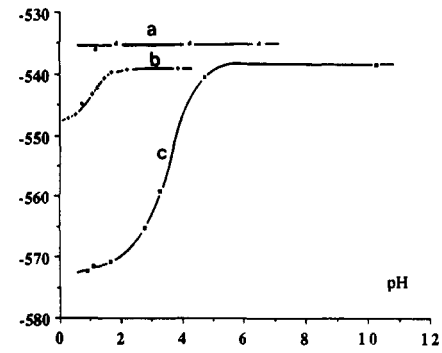

Figure 6. ^{51}V chemical shift versus pH: (a) $H_5[\alpha$-$SiMo_2VW_9O_{40}]$; (b) $H_6[\alpha$-$SiMoV_2W_9O_{40}]$; (c) $H_7[\alpha$-$SiV_3W_9O_{40}]$.

^{51}V NMR Chemical Shifts. All unprotonated vanadium compounds have very similar ^{51}V chemical shifts, i.e. –536, –539, and –540 ppm for the mono- to the trivanadium compounds. For the monoprotonated forms, a shielding of the ^{51}V nucleus by 24 ppm is observed form the mono- to the divanadium compound. An opposite effect was previously observed in the mixed Dawson polyanions,[17] for which the ^{51}V resonance chemical shift increases by about +25 ppm per supplementary vanadium atom. Although no satisfactory explanation can be given now, these opposite trends could be related to the different relative locations of the vanadium atoms in both families: in the Dawson anions they are all located in the same trimetallic group and are connected by edge μ-oxo bridges whereas in the present Keggin anions the adjacent vanadium atoms exchange corner μ-oxo-bridges. The protonation of the anions induces ^{51}V shielding of 8 ppm for α-$[SiMoV_2W_9O_{40}]^{6-}$ and 31 ppm for α-$[SiV_3W_9O_{40}]^{7-}$. pK_a values of about 1 and 3.5 (in 1 M NaCl) can be obtained for these compounds from the variation of δ with pH (Figure 6). It should be noted that ^{183}W chemical shifts depend also on the protonation. In particular, the tungsten atoms adajacent to vanadium undergo large upfield shifts of 15 ppm in the case of the trivanadic compound and 8 ppm (W_5, W_8) and 5 ppm (W_6, W_7) for the divanadic one.

Acknowledgments. The 2D ^{183}W COSY spectrum was recorded during the stay of R.T. at the Laboratorie de Recherches Nord Norsolor (Atochem) in Mazingarbe, France. Henri Strub is gratefully acknowledged for access to the AM 360 Bruker apparatus.

(17) (a) Abbessi, M.; Contant, R.; Thouvenot, R.; Hervé, G. *Inorg. Chem.* **1991**, *30*, 1695. (b) Kozik, M.; Acerete, R.; Hammer, C. F.; Baker, C. W. *Inorg. Chem.* **1991**, *30*, 4429.

(18) Harmalker, S. P.; Leparulo, M. A.; Pope, M. T. *J. Am. Chem. Soc.* **1983**, *105*, 4286. Leparulo-Loftus, M. A.; Pope, M. T. *Inorg. Chem.* **1987**, *26*, 2112.